Research Article

Journal of Physical Organic Chemistry

Received: 9 April 2008, Revised: 19 June 2008, Accepted: 11 July 2008, Published online in Wiley InterScience: 26 August 2008

(www.interscience.wiley.com) DOI 10.1002/poc.1430

Computational (MP2 and DFT) modeling of the substrate/inhibitor interaction with the LDH active pocket in the gas phase and aqueous solution: bimolecular charged (pyruvate/oxamate–guanidinium cation) and neutral adducts (pyruvic/oxamic acids–guanidine)

Ewa D. Raczyńska[a]*, Mariusz Makowski[b], Magorzata Hallmann[a] and Kinga Duczmal[a]

Two types of bimolecular adducts were studied for the substrate and inhibitor of lactate dehydrogenase (LDH), one type of adducts between ionic species, α-keto-carboxylates (pyruvate and oxamate) and the guanidinium cation, and the other type of adducts between neutral species, α-ketocarboxylic (pyruvic and oxamic) acids and guanidine. Calculations were performed in the gas phase and aqueous solution using the MP2 and PCM methods and the 6-31++G basis set. Application of the DFT(B3LYP) and PCM methods led to similar results. A change of the adducts' preference was observed when proceeding from the gas phase to aqueous solution. This change is in good agreement with the acidity–basicity scales in both phases. Formation constant (K_{HB}) for adduct between neutral species is greater for pyruvic than for oxamic acid in the gas phase, whereas a reverse situation takes place in aqueous solution, where the K_{HB} value for adduct between ionic species is smaller for pyruvate than for oxamate. The water molecules favor interactions of more polar oxamate with the guanidinium cation. Stronger interaction with this cation, a model of the arginine fragment of the LDH pocket, suggests that oxamate (inhibitor of LDH) has stronger binding properties in aqueous solution than pyruvate (substrate of LDH). Copyright © 2008 John Wiley & Sons, Ltd.**

Keywords: modeling substrate/inhibitor-LDH interactions; gas phase; water; formation constants; MP2; DFT; PCM; molecular dynamics; umbrella-sampling

INTRODUCTION

Intra- and intermolecular H-bond formation and/or proton transfer play a crucial role in many biological processes.[1–5] For example, they are responsible for the interactions of active molecules with proteins, enzymes, or specific receptors. Depending on the acid-base properties of the binding center, a molecule may gain or lose a proton(s), form intra- or intermolecular H-bond(s) and attain the form and conformation specifically required by the active pocket. Therefore, it is not always evident that the structural preference of a compound is the same in the nanoscopic environment shaped by an active pocket as it is in the gas phase, in the homogeneous aqueous environment, or in the crystal lattice.[6–8] For this reason, investigations for active molecules in various environments have always attracted attention of chemists, biochemists, physicians, *etc*. Since experiments in the native environment are difficult to perform, very often investigations are carried out for the systems which model interactions in living organisms.

α-Ketocarboxylates belong to biologically important metabolites.[9–12] Pyruvate (CH_3COCOO^-, Pyr), the anion of the simplest α-ketocarboxylic acid called pyruvic acid ($CH_3COCOOH$, PyrH), is the metabolite of glucose. It is also the substrate of lactate dehydrogenase (LDH). Oxamate ($H_2NCOCOO^-$, Ox), the anion of oxamic acid ($H_2NCOCOOH$, OxH) and the isosteric and isoelectronic analogue of pyruvate, is a metabolite of some drugs, and also it is an inhibitor of the enzyme LDH. It binds specifically with

* *Correspondence to: E. D. Raczyńska, Department of Chemistry, Warsaw University of Life Sciences, 02-776 Warszawa, Poland.*
E-mail: ewa_raczynska@sggw.pl

a *E. D. Raczyńska, M. Hallmann, K. Duczmal*
Department of Chemistry, Warsaw University of Life Sciences, 02-776 Warszawa, Poland

b *M. Makowski*
Faculty of Chemistry, University of Gdańsk, ul. Sobieskiego 18, 08-952 Gdańsk, Poland

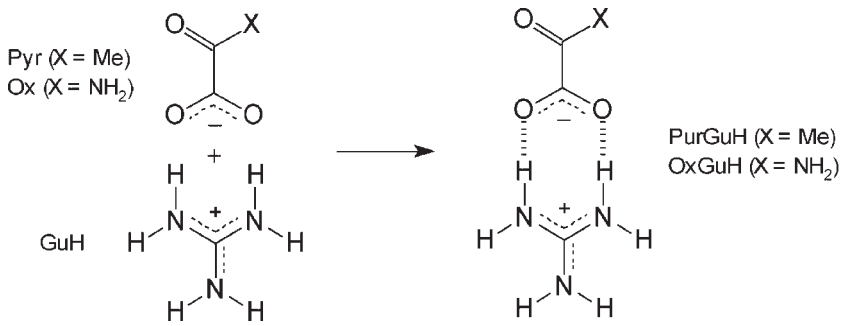

Scheme 1. Formation of bimolecular adducts modeling the substrate/inhibitor-LDH interaction between ionic species

LDH and blocks its active center.[13–15] This property opened new possibilities of applications of oxamate in biotechnology.[16] The NH_2 group of oxamate is chemically more active than the CH_3 group of pyruvate. Hence, oxamate may be used in synthesis of the ligand, modified appropriately for selective bioseparation of LDH[16,17] or in analysis of biomaterials containing LDH.[18–20] Attracted by these applications, we have undertaken systematic studies on geometrical and physicochemical properties of α-ketocarboxylates.[21] In our previous papers, we reported geometrical and physicochemical similarities and differences between these two anions[22–24] and their acids.[25,26] Some discrepancies were observed only for lithium pyruvate.[22,27]

The aim of this work was to study the interactions of the substrate and inhibitor with the simplest and the most active molecule which model the specific interaction with the binding pocket of LDH. These studies are very important for biotechnology, in particular for selective bioseparation of LDH. For the LDH binding pocket, it has been shown that the COO^-/COOH group of the substrate or inhibitor interacts with the guanidinium/guanidine group of the arginine residue (Arg171).[15,28–30] Arginine is the most basic amino acid in the gas phase[31,32] and also in aqueous solution[33] because of its extremely basic guanidine side chain that is predominantly protonated. The Arg residue is very often present in the active sites of many other enzymes.[34,35] However, it is not yet evident, which form, cationic or neutral, takes the guanidine group of the Arg residue in the active pocket of the enzyme, where one or more molecules of water and various polar and nonpolar groups of other amino acids' residues are present.[34] For this reason, we chose two types of bimolecular adducts modeling the interactions of the substrate and inhibitor with the binding pocket of the enzyme LDH: one type of adducts (PyrGuH and OxGuH in Scheme 1) between ionic species, α-ketocarboxylates (Pyr and Ox) and the guanidinium cation (GuH), and the other type of adducts (PyrHGu and OxHGu in Scheme 2) between neutral species, α-ketocarboxylic acids (PyrH and OxH) and guanidine (Gu).

For geometry optimization of isolated acids, their anions, guanidine, the guanidinium cation, and bimolecular charged and neutral adducts, we used the second-order Møller–Plesset perturbation (MP2)[36,37] and density functional theory (DFT)[38] with a combination of the Becke three-parameter hybrid exchange functional with the non-local correlation functional of Lee, Yang and Parr (B3LYP).[39,40] For calculations, the larger basis set 6-31++G** was applied,[41] because investigations of anions, very sensitive to the repulsion between electron-rich groups, and investigations of adducts with intermolecular H-bonds, require diffuse and polarization functions for the C, N, O, and H atoms.[15,21,22–24] Hydrated species (acids, anions,

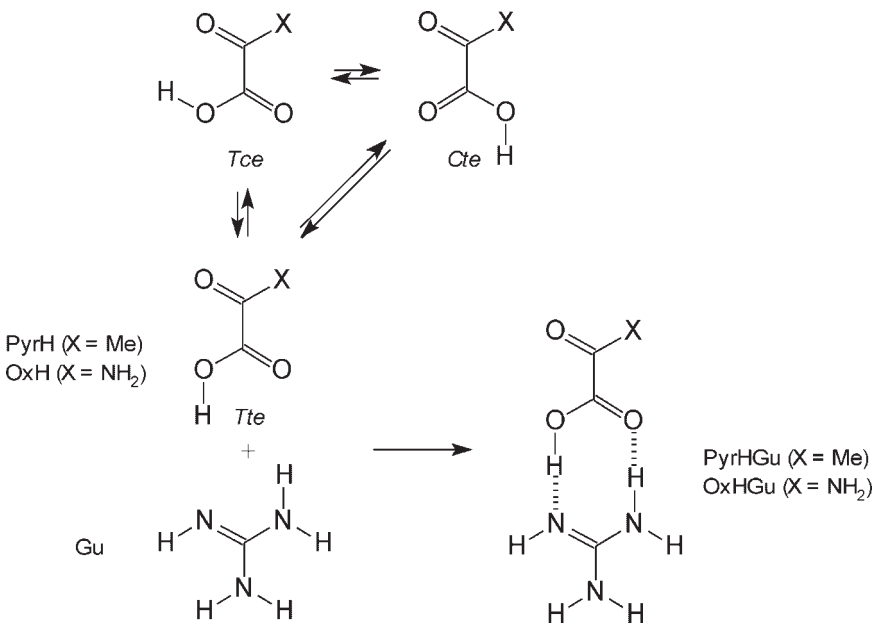

Scheme 2. Formation of bimolecular adducts modeling the substrate/inhibitor-LDH interaction between neutral species

guanidine, guanidinium cation, and adducts) were investigated using the polarizable continuum model {PCM(water)}[42–45] for geometries optimized at the MP2/6-31++G** and DFT(B3LYP)/6-31++G** levels. Formation constants (K_{HB}) were estimated for favored adducts in the gas phase and aqueous solution. Comparison of the calculated K_{HB} values gives the possibility to distinguish similarities and/or differences in binding properties of the substrate and inhibitor in an apolar and polar environment. These properties are essential for the specific interaction with the enzyme LDH. To asses the stability of charged and molecular adducts a series of molecular dynamics simulations were also performed.

METHODS

MP2 and DFT calculations

Geometries of isolated molecules: the pyruvate and oxamate anions, pyruvic and oxamic acids, the guanidinium cation, guanidine, and adducts between neutral and ionic species (Schemes 1 and 2) were fully optimized without symmetry constraints using the MP2[36,37] and DFT(B3LYP) methods[38–40] and the 6–31++G** basis set.[41] For minima (with real frequencies), which correspond to the conformational preferences, the Gibbs free energies ($G = H - TS$) were calculated at 298.15 K using the same level of theory. The G values include changes in the zero-point energy (ZPE) and thermal corrections (vibrational, rotational and translational) to the enthalpy (H) and entropy (S). The BSSE (Basis Set Superposition Error)[46] was calculated using standard computational procedure.[47] The proton-transfer curves for the PyrHGu and OxHGu adducts were calculated by carrying out a series of constrained energy minimization with the O-H distance fixed at a given value and optimizing the remaining degrees of freedom. Both proton transfer curves were calculated using DFT/B3LYP method and the 6-31++G(d,p) basis set. Effect of water molecules was studied using the PCM method[42,45] for geometries optimized at the MP2/6-31++G** and DFT(B3LYP)/6-31++G** levels. The PCM model employs a van der Waals surface type cavity. In this model, the free energy of a solvated system (G_{solv}) is described as a sum over three terms, i.e., electrostatic (G_{elec}), dispersion-repulsion ($G_{disp\text{-}rep}$) contributions to the free energy, and the cavitation energy (G_{cav}). The cavity is defined as a series of interlocking van-der Waals spheres centered at atoms forming a molecule. All calculations were performed using the Gaussian 98 program.[48]

Molecular dynamics simulations

The potentials of mean force (PMFs) were determined by umbrella-sampling molecular dynamics (MD) simulations in explicit water as functions of distance. Sampling of the configurational space, necessary in the umbrella-sampling method, was carried out for the systems involving formation of dimers composed of pyruvate and oxamate with the guanidinium cation (PyrGuH and OxGuH), as well as for those composed of pyruvic and oxamic acids with guanidine (PyrHGu and OxHGu). A series of umbrella-sampling molecular dynamics simulations with the AMBER force field was carried out for each pair using the TIP3P[49] water model. The dimers were immersed in TIP3P water boxes with periodic boundary conditions with a box side of about 35,35,35, and 33 Å for PyrGuH, OxGuH, PyrHGu, and OxHGu, respectively. Molecular dynamics simulations were carried out in two steps. In the first step, each system was equilibrated in the NPT ensemble (constant number of particles, pressure, and temperature) at 298 K for 100 ps. Production MD simulations were then run in the NVT ensemble (constant number of particles, volume, and temperature). In all MD simulations, the integration step was 2 fs. A 9 Å cut-off was used for all non bonded interactions, and the electrostatic energy was evaluated using the particle-mesh Ewald summation.[50] For each system, a series of 19 windows of 4 ns simulations per window was run with different harmonic-restraint potentials imposed on the distance (i) between the two atoms (one from each particle) closest to the geometric center of the molecules, as given by Eqn (1).

$$V(\xi) = k(\xi - d_o)^2 \quad (1)$$

with the force constant $k = 2$ kcal mol^{-1} Å^{-2} and the 'equilibrium' distance (d_o) for a given window equal to 3.0, 3.5, 4.0, . . ., 12.0 Å for every dimer studied in this work, for windows from 1 to 19. Snapshots from the MD simulations were saved every 0.2 ps. A total number of 20 000 configurations were collected for each window.

The charges on the atoms of the solute molecules needed for the AMBER 7.0[51] force field were determined for each system using a standard procedure for fitting the point-charge electrostatic potential to the molecular electrostatic potential computed by using the electronic wave function calculated at the restricted Hartree-Fock (RHF) level with the 6–31 G* basis set. The program GAMESS[52] was used to carry out the quantum-mechanical calculations, while the program RESP[53] of the AMBER 7.0 package was used to compute the fitted charges. The charges and the AMBER atom types are shown in Fig. 1.

The potentials of mean force (PMFs) were calculated using the weighted histogram analysis method (WHAM).[54,55] To determine the PMFs for the systems studied, we processed the results from all windows of the restrained MD simulations for each system, for which one-dimensional histograms, dependent only on the distance between the geometric centers of interacting dimers, were constructed. This means that our PMF plots were averaged over all possible orientations. The bin dimension applied in the WHAM calculations of the PMF was equal to 0.1 Å for all systems.

RESULTS AND DISCUSSION

Geometries of the anionic and neutral forms of the substrate and inhibitor of LDH

The MP2 and DFT structures of isolated pyruvate and oxamate (Pyr and Ox) and their acids (PyrH and OxH) were described previously.[21–26] Both methods predict similar structures for isolated species: twisted structures for anions (more twisted for pyruvate than oxamate) and almost planar structures for acids (*Tce*, *Tte*, and *Cte* given in Scheme 2). The X-ray structures for anions are also slightly different: pyruvates are twisted, whereas those of oxamates are planar.[56–60] For acids, the same stable conformations were found at other levels of theory.[21,25,26,61,62] Their nomenclature were taken from reference. [61]. Among them the *Tce* structure, stabilized by the intramolecular H-bond between the $^{\alpha}$CO and OH groups, is favored in the gas phase.[21,25,26,61–68] Other structures, *Tte* and *Cte*, have greater energies than that of *Tce* (by 1–3 and 2–4 kcal mol^{-1}, respectively).[21,25,26,61,62] They predominate for the associated

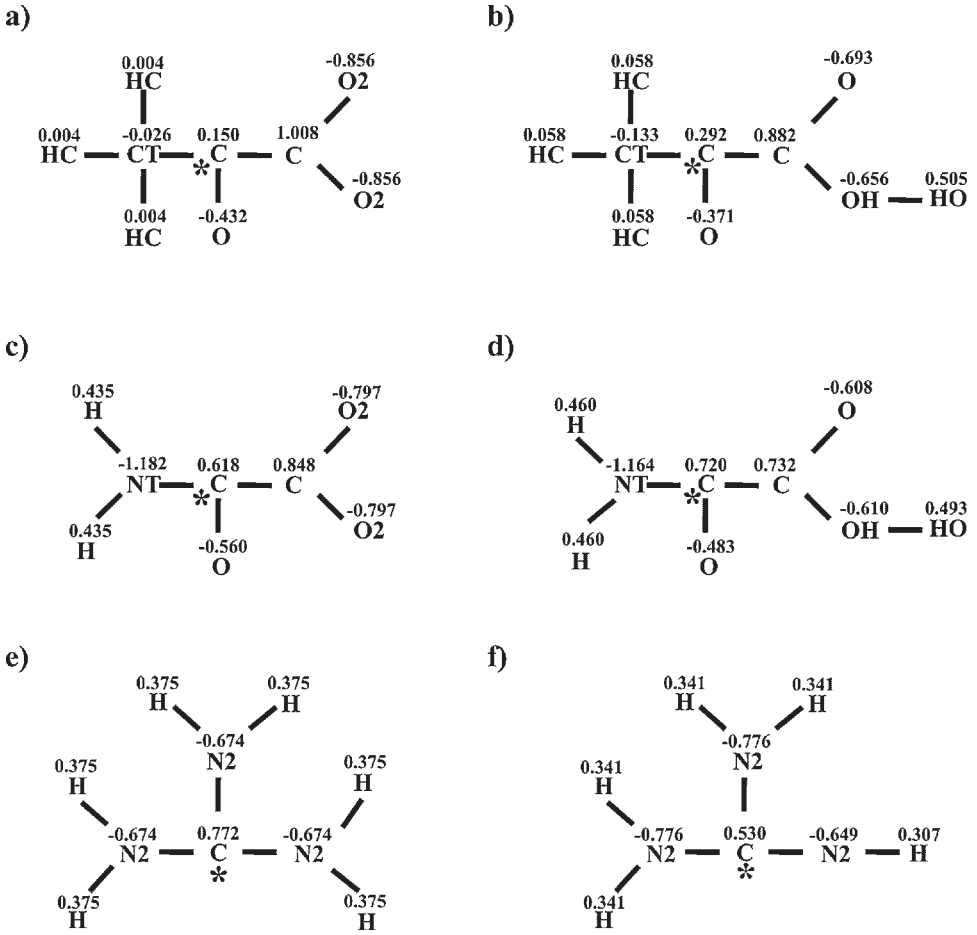

Figure 1. Partial atomic charges (in electron charge units) of the Pyr (a), PyrH (b), Ox (c), OxH (d), GuH (e), and Gu (f) molecules calculated by using the RESP method[53] based on HF/6-31G* calculations carried out with GAMESS[52] used in the calculations with the AMBER force field.[51] The atoms are labeled with standard AMBER atom-type symbols. The restraints during the MD simulations were imposed at the distances between the atoms labeled with stars

forms in the gas phase, solution, and solid state.[61,69–72] Selected geometrical parameters calculated at the MP2/6-31++G(d,p) level for the pyruvate and oxamate anions and their acids are given in Tables 1 and 2, respectively. Besides geometry, polarity of the substrat and inhibitor may also influence their interactions with the binding pocket of LDH. Interestingly, the MP2 (or DFT) calculated dipole moment (μ) for pyruvate is only slightly smaller than that for oxamate (Table 1). Similarly, the calculated μ value for the *Tte* structure of pyruvic acid is smaller than that for the same structure of oxamic acid (Table 2). The μ value of the *Tce* structure of pyruvic acid (2.74 and 2.52 D at the DFT and MP2 levels, respectively) is very close to the experimental one (2.30 ± 0.03 D).[73] The same trends were observed when other quantum-chemical methods were applied.[15,21–26,61–68]

Tautomeric forms of both anions, the enol form of pyruvate {$H_2C{=}C(OH)COO^-$} and the iminol form of oxamate {$HN{=}C(OH)COO^-$}, have considerably higher Gibbs free energies than the corresponding keto (Pyr) and amide (Ox) forms (by more than 5 and 4 kcal mol^{-1}, respectively at the B3LYP/6-31++G** level[24]). Similarly, the enol form of pyruvic acid {$H_2C{=}C(OH)COOH$} and the iminol form of oxamic acid {$HN{=}C(OH)COOH$}, have considerably higher Gibbs free energies than the corresponding keto (PyrH-*Tte*) and amide (OxH-*Tte*) forms (by more than 5 and 10 kcal mol^{-1}, respectively at the same level of theory[21,25,26]). Consequently, they were not taken into account in this paper.

Geometries of the cationic and neutral forms of the LDH active center model

Geometries of guanidine (Gu) and its cation (GuH) – models of the arginine fragment of the LDH pocket – were previously discussed.[74,75] The structure of guanidine has not been experimentally determined, from either X-ray diffraction, electron diffraction or microwave spectra. Some experimental information on its structure has only been obtained from the infrared spectrum of guanidine in the solid state.[76] From the analysis of this spectrum, it was suggested that guanidine prefers to adopt a planar conformation. However, the MP2 and DFT calculations showed that the planar conformation of guanidine has three imaginary frequencies. Two stable non-planar structures of guanidine were found with very close energies. They differ by only 1–2 kcal mol^{-1}. Both methods (MP2 and DFT) predict similar angles and bond lengths.

In the case of the guanidinium cation, only non-planar structure (with the NH_2 groups rotated out of the CN_3 plane by 16°) was found at both levels of theory. Completely planar structure has three imaginary frequencies. The structure of the

Journal of Physical Organic Chemistry

Table 1. Selected geometrical parameters (CX bond lengths in Å, angles in degree) and dipole moments (μ in Debyes) calculated at the MP2/6-31++G** level for α-ketocarboxylates (Pyr and Ox), the guanidinium cation (GuH), and their bimolecular charged adducts (pyrguh and oxguh)

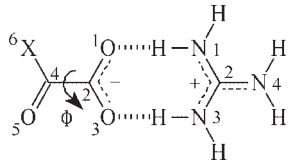

PyrGuH (X = Me)
OxGuH (X = NH_2)

Property	Pyr	Ox	GuH	PyrGuH	OxGuH
Anion					
C2O1	1.270	1.277	—	1.291	1.280
C2O3	1.264	1.254	—	1.246	1.263
C4O5	1.238	1.238	—	1.237	1.232
C2C4	1.532	1.571	—	1.545	1.547
O1C2O3	131.3	130.7	—	129.0	127.3
Φ	76.3	−20.0	—	−30.2	−14.3
Guanidinium cation					
C2N1	—	—	1.336	1.333	1.330
C2N3	—	—	1.336	1.325	1.325
C2N4	—	—	1.336	1.366	1.371
N1C2N3	—	—	120.0	119.6	120.2
H-bond					
C2O1···HN1 (GH)	—	—	—	1.545	1.539
C2O3···HN3 (GH)	—	—	—	1.645	1.582
μ	5.95	5.99	0.00	9.69	11.53

guanidinium cation has been experimentally determined for numerous salts and complexes. All data have been compiled in the Cambridge Structural Database.[77,78] Generally, the CN_3 moiety is planar and the CN bond lengths are equal (within experimental errors). Unfortunately, the X-ray analysis does not give reliable data on the position of the hydrogen atoms, and no more informations can be derived for the structure of the guanidinium cation from experiments performed in the solid state.[74,75] Selected geometrical parameters calculated at the MP2/6-31++G(d,p) level for the guanidinium cation and guanidine are given in Tables 1 and 2, respectively.

Geometries of adducts modeling the interaction of the substrate/inhibitor with the binding pocket of LDH

The structures for bimolecular charged adducts of α-ketocarboxylates with the guanidinium cation (PyrGuH and OxGuH) and for bimolecular neutral adducts of α-ketocarboxylic acids with guanidine (PyrHGu and OxHGu), optimized at the MP2/6-31++G(d,p) level, are given in Figs. 2 and 3, respectively. The pyruvate and oxamate anions interact non-covalently with the guanidinium cation in PyrGuH and OxGuH, and form cyclic dimers with two intermolecular H-bonds between the charged COO^- and $C(NH)_2^+$ groups. Similarly, pyruvic and oxamic acids interact non-covalently with guanidine in PyrHGu and OxHGu, and form cyclic dimers with two intermolecular H-bonds between the neutral COOH and $C(NH)NH_2$ groups. The intermolecular H-bond distances are given in Tables 1 and 2. The intramolecular interactions for isolated anions and acids were discussed previously.[21–25,79] Thermodynamic parameters, such as electronic energy (*E*), zero-point vibrational energy (ZPVE), enthalpy (*H*), entropy (*S*), and Gibbs free energy (*G*) calculated at the MP2/6-31++G(d,p) and DFT/6-31++G(d,p) levels for both types of bimolecular adducts are given in Table 3. To check the level of convergence of calculations, we also present results of single-point calculations performed with the 6-311++G** basis set. The difference between energies is smaller than 0.1% at both levels (DFT and MP2). This means that energies for the systems studied in this work converged very well using the 6-31++G** basis set.

Comparison of the selected geometrical parameters calculated at the MP2/6-31++G(d,p) level (Tables 1 and 2) for isolated molecules: pyruvic and oxamic acids (PyrH-*Tte* and OxH-*Tte*), their anions (Pyr and Ox), guanidine (Gu), its cation (GuH), and bimolecular adducts between the charged (PyrGuH and OxGuH) and neutral species (PyrHGu and OxHGu) shows some interesting trends. The pyruvate and oxamate anions take the twisted conformations for the PyrGuH and OxGuH adducts, similarly as for free anions (Pyr and Ox). However, the dihedral angles $O^{\alpha}CCO$ for PyrGuH (−30°) and OxGuH (−14°) are considerably smaller than those for Pyr (76°) and Ox (−20°). Due to an engagement of the carboxylate COO^- group in the intermolecular H-bonds, the repulsion between the carbonyl $^{\alpha}CO$ and the carboxylate CO group is reduced for adducts in comparison to that for free anions.

Quite a different situation occurs for pyruvic and oxamic acids in their bimolecular adducts with guanidine (PyrHGu and

Table 2. Selected geometrical parameters (CX bond lengths in Å, angles in degree) and dipole moments (μ in Debyes) calculated at the MP2/6-31++G** level for α-ketocarboxylic acids (PyrH-*Tte* and OxH-*Tte*), guanidine (Gu), and their bimolecular neutral adducts (PyrHGu and OxHGu)

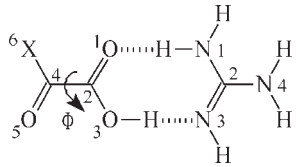

PyrHGu (X = Me)
OxHGu (X = NH_2)

Property	PyrH-*Tte*	OxH-*Tte*	Gu	PyrHGu	OxHGu
Acid					
C2O1	1.224	1.225	—	1.241	1.243
C2O3	1.346	1.341	—	1.310	1.305
C4O5	1.226	1.229	—	1.227	1.230
C2C4	1.538	1.536	—	1.537	1.540
O1C2O3	124.8	124.9	—	126.7	126.7
Φ	0.1	−7.4	—	25.3	−9.2
Guanidine					
C2N1	—	—	1.394	1.369	1.370
C2N3	—	—	1.288	1.300	1.300
C2N4	—	—	1.400	1.389	1.388
N1C2N3	—	—	120.2	120.7	120.7
H-bond					
C2O1···HN1 (G)	—	—	—	1.935	1.933
C2O3···HN3 (G)	—	—	—	1.565	1.555
μ	1.52	2.52	3.07	6.28	6.97

OxHGu). An engagement of the carboxylic hydrogen atom in the intermolecular H-bond for PyrHGu and OxHGu augments the electron density of the carboxylic oxygens and increases the repulsion between the electron-rich CO groups in comparison to that for free acids (PyrH-*Tte* and OxH-*Tte*). Therefore, the two acids take slightly twisted conformations for bimolecular neutral adducts. The dihedral angles $O^{\alpha}CCO$ for acids in their adducts PyrHGu (25°) and OxHGu (−9°) are greater than those for free acids PyrH-*Tte* (0°) and OxH-*Tte* (−7°). However, these angles for neutral adducts (PyrHGu and OxHGu) are smaller than those for charged adducts (PyrGuH and OxGuH).

Due to intramolecular X···OC interactions, the carboxylate CO bonds of anions for the PyrGuH and OxGuH adducts have not the same lengths, similarly as those for the free Pyr and Ox anions (Table 1). Consequently, the CN bonds of the guanidinium cation and the intermolecular H-bonds ($NH^{+}\cdots{}^{-}OC$) are not equivalent for charged adducts. The shorter carboxylate CO bond forms the longer intermolecular H-bond. Differences between the CO bond lengths vary when going from the free to associated species in higher degree for pyruvate (from 0.006 to 0.045 Å) than for oxamate (from 0.023 to 0.017 Å). Difference between the intermolecular H-bonds for the pyruvate adduct (0.100 Å) is also greater than that for the oxamate adduct (0.043 Å). These differences are parallel to the variations of the dihedral angle $O^{\alpha}CCO$ which are greater for pyruvate than for oxamate.

Protonation of the α-ketocarboxylate anions and deprotonation of the guanidinium cation reduce π-electron delocalization in the carboxylic COO and guanidine CNN moieties, respectively, and increase differences between the CO and CN bond lengths (Table 2). On the other hand, the intermolecular H-bonds present for the PyrHGu and OxHGu adducts increase π-electron delocalization in the COO and CNN moieties. Consequently, differences between the CO bond lengths are twice smaller for associated than free acids. When going from the free to associated species, they vary in slightly higher degree for pyruvate (from 0.122 to 0.069 Å) than for oxamate (from 0.116 to 0.062 Å). The two intermolecular H-bonds between the neutral O═C—OH and N═C—NH groups are also more differentiated for PyrHGu and OxHGu than those between the charged COO^{-} and $C(NH)_2^{+}$ groups for PyrGuH and OxGuH. The H-bonds between the OH and C═N groups (OH···N═C) are longer than those between the NH and C═O groups (C═O···HN) by *ca.* 0.4 Å for PyrHGu and OxHGu. For comparison, differences between the H-bonds ($NH^{+}\cdots{}^{-}OC$) for PyrGuH and OxGuH are not larger than 0.1 Å.

Great variations of the dihedral angle $O^{\alpha}CCO$ for anions cause also significant changes for the central CC bond when proceeding from the free to associated species. Differences between the CC bond lengths for free and associated pyruvate (0.013 Å) and oxamate (0.024 Å) are higher than those for free and associated pyruvic (0.001 Å) and oxamic acids (0.004 Å). However, the dihedral angle $O^{\alpha}CCO$ and the intramolecular H-bonds present in bimolecular adducts have small influence on the $^{\alpha}CO$ bond lengths. Their changes do not exceed 0.01 Å. Variations of the OCO and NCN angles are not larger than 4°. Relative polarities of bimolecular adducts are similar to those of free anions and acids (Tables 1 and 2). The MP2 calculated dipole moment for

Journal of Physical Organic Chemistry

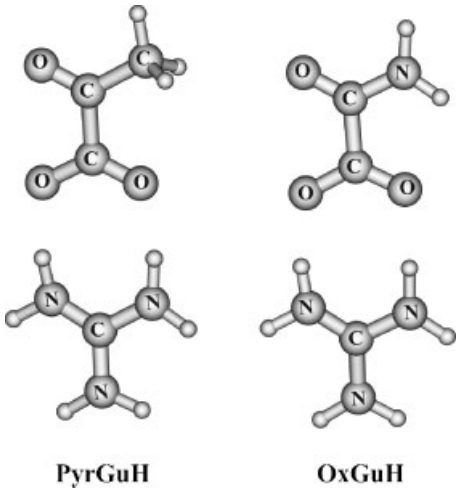

Figure 2. MP2/6-31++G(d,p) structures of bimolecular charged adducts between α-ketocarboxylates and the guanidinium cation (PyrGuH for pyruvate and OxGuH for oxamate)

PyrGuH (9.69 D) is smaller than that for OxGuH (11.53 D), and also the MP2 calculated dipole moment for PyrHGu (6.28 D) is smaller than that for OxHGu (6.97 D).

Similar structures for charged (PyrGuH and OxGuH) and neutral (PyrHGu and OxHGu) adducts, and similar differences in their geometrical parameters and polarities were found at the DFT(B3LYP)/6-31++G(d,p) level.[79] Generally, the DFT calculated H-bonds are shorter than the MP2 ones (by no more than 0.01 Å for charged adducts, and by 0.04–0.07 Å for neutral adducts). The DFT calculated dihedral angles $O^{\alpha}CCO$ for associated anions and acids are smaller than the MP2 ones. However, the observed trend is the same, the $^{\alpha}CO$ group is twisted out of the COO^{-} plane in higher degree for pyruvate (-20.4°) and pyruvic acid (1.9°) than for oxamate (-0.1°) and oxamic acids (-0.4°). Differences in the other angles calculated at the MP2 and DFT levels are not larger than 1°. Differences in the bond lengths calculated at the MP2 and DFT levels are not larger than 0.02 Å. Generally, the DFT calculated CO bond lengths are slightly shorter than the MP2 ones, and the DFT calculated central CC bond lengths are slightly longer than the MP2 ones, similarly as for free acids and their anions. The calculated dipole moment for PyrGuH (10.41 D) is smaller than that for OxGuH (10.99 D), and also the calculated dipole moment for PyrHGu (6.66 D) is smaller than that for OxHGu (7.15 D).

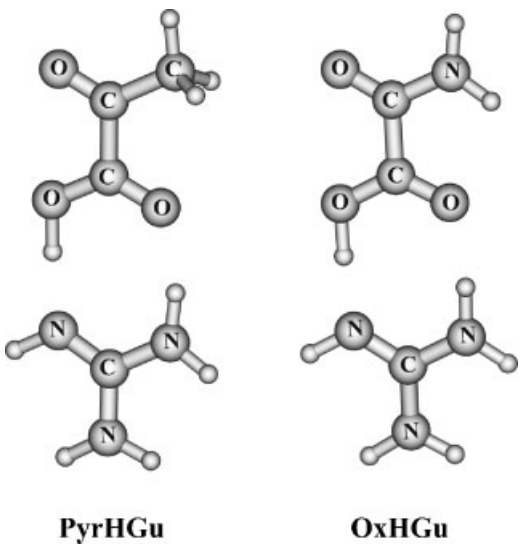

Figure 3. MP2/6-31++G(d,p) structures of bimolecular neutral adducts between α-ketocarboxylic acids and guanidine (PyrHGu for pyruvic acid and OxHGu for oxamic acid)

The non-covalent interactions of the COO^{-} and the $C(NH)_2^{+}$ groups were experimentally studied in the solid state for benzamidinium pyruvate.[80] For this adduct, pyruvate has the twisted conformation, and the dihedral angle $O^{\alpha}CCO$ is equal to 5.2°. The carboxylate CO and the amidinium CN bonds are not equivalent. Their lengths differ by 0.005 and 0.007 Å, respectively. Consequently, the $CO^{-}\cdots{}^{+}HN$ bonds have not the same lengths. They differ by 0.013 Å. Similar differences in the bond lengths were observed for crystal methylguanidinium formate.[81] It is interesting to mention here that linear bidentate H-bonding between the guanidinium and the carboxylate groups were reviewed for the crystal structures of various guanidinium–carboxylate derivatives.[82] The guanidinium–carboxylate interactions were also studied for crystal structures of arginine peptides[83] and proteins.[84]

Relative stabilities of bimolecular adducts in the gas phase and aqueous solution

For bimolecular charged adducts of the pyruvate and oxamate anions with the guanidinium cation (PyrGuH and OxGuH), and for bimolecular neutral adducts of pyruvic and oxamic acids with guanidine (PyrHGu and OxHGu), the total electronic energies (E) were calculated for the isolated species (in the gas phase) at the MP2/6-31++G** level and separately for the solvated species (in aqueous solution) at the PCM(water)//MP2/6-31++G** level. For comparison, calculations were also performed at the B3LYP/6-31++G** and PCM(water)//B3LYP/6-31++G** levels, respectively. Next, the E values for charged adducts (PyrGuH and OxGuH) were compared with those for neutral adducts (PyrHGu and OxHGu). The relative total energies {$\Delta E = E$(charged adduct) E(neutral adduct)}, calculated for both the isolated and hydrated adducts, are listed in Table 4. It should be mentioned here that in systems consisting of at least two monomers (dimer or higher adduct), the calculated interaction energy is decreased due to the fact that the basis set of complex formed is artificially enlarged with respect to basis sets of the monomers. This causes en error called Basis Set Superposition Error (BSSE).[46] To compute the BSSE, the standard procedure was applied.[47] The MP2 method gives slightly larger BSSE (3.8 kcal mol^{-1} for charged adducts and 3.1–3.2 kcal mol^{-1} for neutral adducts) than the B3LYP method (0.8–0.9 and 1.0 kcal mol^{-1}, respectively). However, this does not change general trend for adducts' stability (Table 4).

Generally, the DFT results are similar to the MP2 ones. Bimolecular neutral adducts (PyrHGu and OxHGu) have smaller energies in the gas phase, whereas bimolecular charged adducts (PyrGuH and OxGuH) have smaller energies in aqueous solution. Water molecules favor the transfer of the proton from α-ketocarboxylic acid to guanidine and stabilize interactions between the ions, α-ketocarboxylates and the guanidinium cation (Scheme 3). In the gas phase, interactions between the neutral acids and guanidine are preferred. These trends are in good agreement with the acidity–basicity scales found in the gas phase and aqueous solution.[85] For comparison, amino acids prefer their neutral forms in the gas phase (or apolar

Table 3. Electronic energies (*E*), zero-point vibrational energies (ZPVE), enthalpies (*H*), entropies (*S*) and Gibbs free energies (*G*) for charged (PyrGuH and OxGuH) and neutral (PyrHGu and OxHGu) adducts calculated at the MP2 and DFT levels (in parentheses are energies for single-point calculations performed using the 6-311++G** basis set)

Adduct	E^a	ZPVE[b]	H^a	S^c	G^a
		a) MP2/6-31++G**			
PyrGuH	−546.318063 (−546.519576)	94.31	−546.154487	112.31	−546.207850
OxGuH	−562.372662 (−562.595665)	87.43	−562.220663	110.28	−562.273062
PyrHGu	−546.324542 (−546.534943)	94.59	−546.160830	111.90	−546.213999
OxHGu	−562.372906 (−562.598373)	88.02	−562.220148	108.69	−562.271789
		b) B3LYP/6-31++G**			
PyrGuH	−547.844480 (−547.970973)	92.28	−547.683760	115.07	−547.738433
OxGuH	−563.919934 (−564.062412)	85.68	−563.770449	110.21	563.822813
PyrHGu	−547.850917 (−547.986855)	92.45	−547.690529	112.04	−547.743762
OxHGu	−563.918258 (−564.061042)	86.18	−563.768361	107.95	−563.819653

[a] In Hartree, 1Hartree = 627.5095 kcal mol^{-1}.
[b] In kcal mol^{-1}.
[c] In cal deg^{-1} mol^{-1}.

environment), whereas in aqueous solutions (or polar environment) they exist in their ionic forms (*e.g.*, zwitterionic forms at neutral pH).[86] Since it is not yet evident, which form, cationic or neutral, takes the guanidine group of the Arg residue in the active pocket of the LDH enzyme, the results for both types of adducts (neutral and charged) should be considered.

Proton transfer for bimolecular adducts in the gas phase

The potential energy surface for the proton transfer in the neutral adducts PyrHGu and OxHGu with formation of the charged adducts PyrGuH and OxGuH may have a different character: a double- or a single-well. To characterize its shape, we examined the proton-transfer curves at the DFT(B3LYP)/6-31++G(d,p) level. These curves are qualitatively similar with very low energy barriers between the first and the second minima being 0.36 and 0.21 kcal mol^{-1} for PyrHGu (Fig. 4a) and OxHGu (Fig. 4b), respectively. Their shapes are very characteristic for the usual H-bond between neutral acid and neutral base.[87] The proton is preferentially located on the carboxylate group in the gas phase.

Table 4. Comparison of the relative energies (ΔE in kcal mol^{-1})[a] between charged and neutral adducts in the gas phase and aqueous solution using the PCM model calculated at the MP2 and DFT levels

		ΔE	
Pair of adducts	Method	Gas phase	Water (PCM)
PyrGuH/PyrHGu	MP2/6-31++G**	4.1 (4.7)[b]	−8.9
	B3LYP/6-31++G**	4.0 (3.9)[b]	−7.6
OxGuH/OxHGu	MP2/6-31++G**	0.2 (0.7)[b]	−9.5
	B3LYP/6-31++G**	1.1 (1.3)[b]	−10.1

[a] $\Delta E = E$(charged adduct) – E(neutral adduct).
[b] $\Delta(E + \text{BSSE})$ given in parentheses.

Potentials of mean forces (PMFs) in water

For determinations of the PMF curves for the charged and neutral adducts which model the substrat/inhibitor-LDH interactions, we applied the MD simulations using the umbrella-sampling/WHAM method with the TIP3P water model. Figure 5 shows the dependence of the PMF for the charged adduct OxGuH, obtained on the number of configurations collected from each window. As seen from the figure, convergence is achieved as the number of configurations increases. The same convergence was observed for the remaining dimers.

Results of the PMF calculations for the charged adducts PyrGuH (dashed line) and OxGuH (solid line) are given in Fig. 6. The PMF curves have characteristic shapes with one deep minimum each at about 5.4 and 5.2 Å, corresponding to PyrGuH and OxGuH, respectively. This minimum is referred to the contact minimum. The deepest contact minima are observed for the PyrGuH (dashed line) adduct with depths of about −1.6 kcal mol^{-1}, and being about 0.2 kcal mol^{-1} lower that for the OxGuH adduct. The PMF curves shown in Fig. 6 also contain the second minima at distances of about 7.5 Å. These so-called solvent-separated minima correspond to the distances at which precisely one water molecule can enter the space between the two solutes. The first maximum in the PMF curve between the contact and solvent-separated minima is referred to the desolvation maximum. In both cases, the maxima are slightly observed.

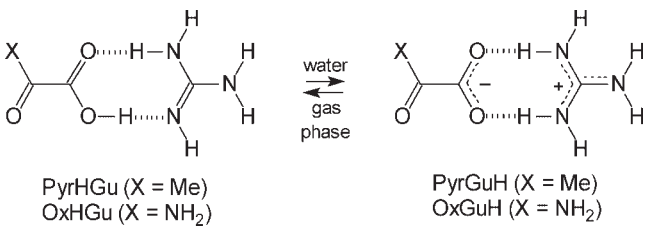

Scheme 3. Transfer of the proton for bimolecular adducts when proceeding from the gas phase to aqueous solution

Journal of Physical Organic Chemistry

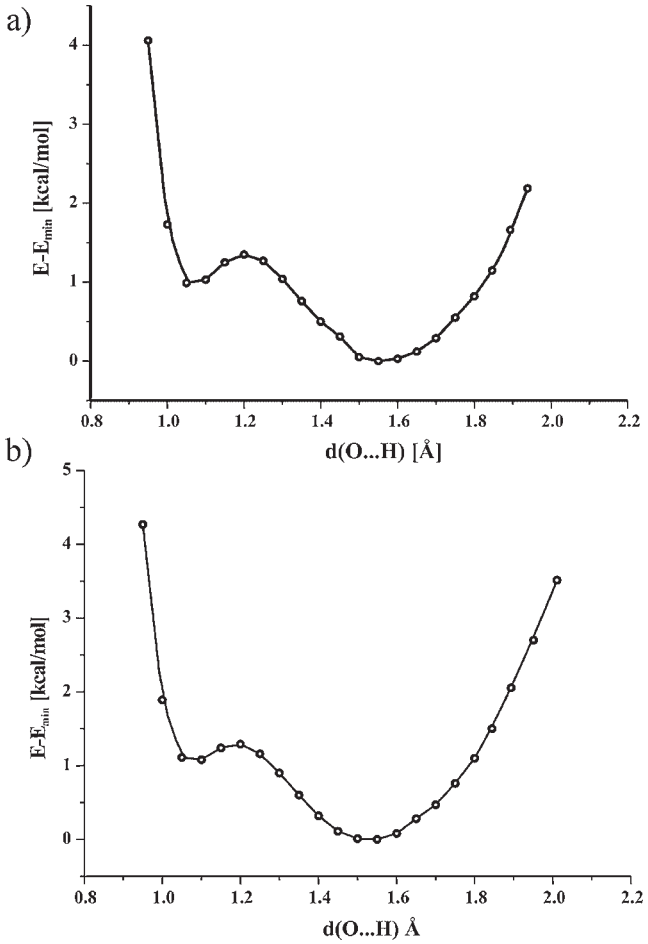

Figure 4. Energy variation on the proton transfer in the O–H···N bridge of the PryHGu (a) and OxHGu (b) adducts. Filled circles represent points where the DFT(B3LYP)/6-31++G** energies have been calculated

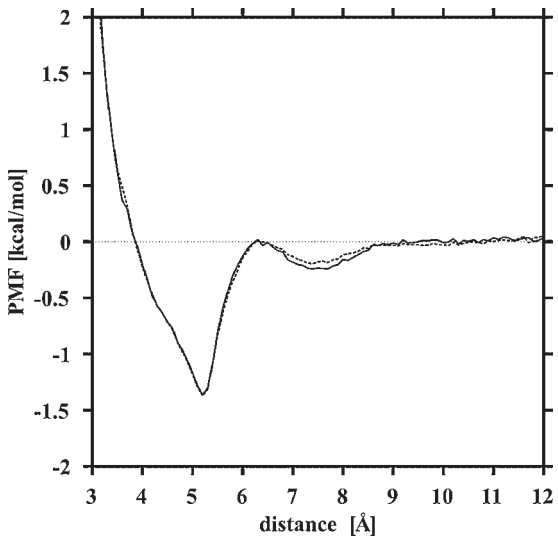

Figure 5. PMF curves for the OxGuH adduct for two different numbers of configurations, obtained from the umbrella-sampling/WHAM method using the TIP3P water model. The simulations were carried out at a temperature of 298 K. The dashed and solid lines refer to 50% (10 000 configurations) and 100% (20 000 configurations), respectively, of the total number of generated configurations

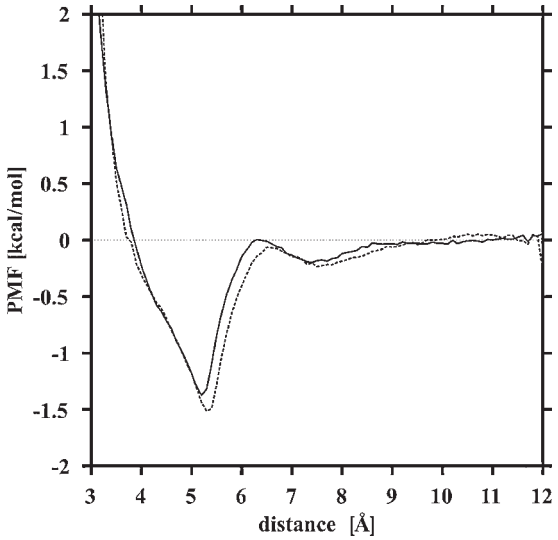

Figure 6. PMF curves determined by using the TIP3P model of water for two charged adducts systems: PyrGuH (dashed line) and OxGuH (solid line)

Masunov *et al.*[88] calculated the PMF profiles for the charged system dependent on orientation – adduct between the propionate anion and the 1-propylguanidine cation. The depth of the minimum of their system calculated for the head-to-head orientation is about −4.5 kcal mol^{-1}, while our values are only −1.4 and −1.6 kcal mol^{-1} for the PyrGuH and OxGuH adducts, respectively. This discrepancy can be attributed to the fact that the orientation of the interacting species in their work was constrained, while in our calculations the orientation was not restricted, and the PMFs profiles were computed over all orientations. The depth of the contact minimum of the PMF curve for the charged adduct between the acetate anion and the 1-methylguanidinum cation, calculated over all orientations by Makowska *et al.*,[89] is only −0.53 kcal mol^{-1}. The difference between our and their results can be caused by the fact that our PMFs were computed between the geometric centers of molecules within the dimer. Chipot at el.[90] calculated the potential of mean force for the charged adduct between the guanidinium and acetate ions in water. They found a contact minimum at 4.1 Å and a broad solvent-separated minimum at 6.4 Å.

We can assume that Pyr, Ox, and GuH consist at least of two parts, i.e., charged and hydrophobic. Based on that assumption it could be found that our PMFs shown in Fig. 6 are a sum over three types of solute–solute interactions (dependent on orientation), i.e., hydrophobic–hydrophobic, hydropbobic–charged, and charged–charged. The deepest minima in the PMF curves reported in the literature[88,90,91] are observed for the charged–charged interaction. This allows us to state that the most dominating structures of the PyrGuH and OxGuH adducts are those with the charged parts of molecules orientated with respect to each other.

Figure 7 shows the results of the PMF calculations for the PyrHGu (dashed line) and OxHGu (solid line) adducts. The PMF curves have one wide depth with two minima at about 3.4 and 5.0 Å, and 3.6 and 5.2 Å corresponding to PyrHGu and OxHGu, respectively. There is a very low energy barrier between the minima being about 0.25 and 0.10 kcal mol^{-1} corresponding to PyrHGu and OxHGu, respectively. The presence of these two

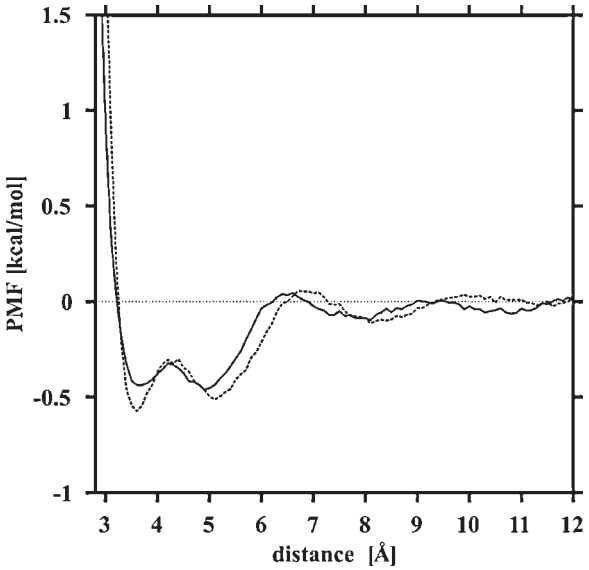

Figure 7. PMF curves determined by using the TIP3P model of water for two molecular dimer systems: PyrH-Gu (dashed line) and OxH-Gu (solid line)

minima in PMF profile can be contributed to the fact that there are two possible hydrogen bonds in the systems consisting of pyruvic acid – guanidine and oxamic acid – guanidine. These molecular systems can be stabilized by the following hydrogen bonds between C═O···H—NH and O—H···NH═, where the hydrogen bond forms between the oxygen atom in the carbonyl group of pyruvic or oxamic acid and the hydrogen atom of one of the amine group of guanidine, or between the hydrogen atom in the hydroxyl group of pyruvic or oxamic acid and the nitrogen atom of the imino group of guanidine. Similarly as for PMFs in Fig. 6, we can assume that PyrH, OxH, and Gu consist at least of two parts, i.e., polar and hydrophobic. PMFs shown in Fig. 7 are a sum over three types of solute–solute interactions (dependent on orientation), i.e., hydrophobic–hydrophobic, hydropbobic–polar, and polar–polar. For these types of interactions we can distinguish three dominating orientations of polar pairs studied in this work, i.e., side-to-side (paralell, antiparallel), side-to-edge or edge-to-side (perpendicular), and edge-to-edge (when systems lie in the same line). The distances between the centers of interacting molecules increase from parallel to edge-to-edge positions.[92] This means that these two minima in the curves present in Fig. 7 refer to side-to-side (at the shortest distance) and edge-to-edge (at the longest distance) positions.

The depth of the contact minima for the PyrH-Gu (dashed line) and OxH-Gu (solid line) dimers are about −0.6 and −0.45 kcal mol^{-1}, respectively. The PMF curves shown in Fig. 7 contain also the second minima at distances of about 8.0 Å. The so-called solvent-separated minima correspond to the distances at which precisely one water molecule can enter the space between the two solutes. These minima are deeper than those observed in Fig. 6.

Formation constants for bimolecular adducts

The Gibbs free energies calculated at 298.15 K for α-ketocarboxylic acids, their anions, guanidine, its cation, and both types of bimolecular adducts were used to estimate the Gibbs free energies for the formation of adducts (G_{HB}) and next to calculate the formation constants (K_{HB}). For isolated neutral adducts between α-ketocarboxylic acids (PyrH and OxH abbreviated as AH) and guanidine (Gu abbreviated as B), favored in the gas phase, the G_{HB} values were calculated at the MP2/6-31++G**//MP2/6-31++G** and DFT(B3LYP)/6-31++G**//DFT(B3LYP)/6-31++G** levels for equilibrium (2) according to Eqn (3). For hydrated charged adducts between the α-ketocarboxylate anions (Pyr or Ox abbreviated as A^-) and the guanidinium cation (GuH abbreviated as BH^+), favored in aqueous solution, the G_{HB} values were calculated at the PCM(water)//MP2/6-31++G** and PCM(water)//DFT(B3LYP)/6-31++G** levels for equilibrium (4) according to Eqn (5). To calculate the free energy changes (ΔG_{HB}) of the systems studied in water, the PCM model was used for the geometries optimized at the MP2/6-31++G** and DFT(B3LYP)/6-31++G** levels, respectively. The K_{HB} values for isolated and hydrated adducts were estimated using relation (6).

$$AH + B \rightleftarrows AH:::B \quad (2)$$

$$\Delta G_{HB} = G(AH:::B) - G(AH) - G(B) \quad (3)$$

$$A^- + BH^+ \rightleftarrows A^-:::{}^+HB \quad (4)$$

$$\Delta G_{HB} = G(A^-:::{}^+HB) - G(A^-) - G(BH^+) \quad (5)$$

$$K_{HB} = \exp\left(\frac{-\Delta G_{HB}}{RT}\right) \quad (6)$$

Table 5 summarizes the ΔG_{HB} and K_{HB} values estimated for neutral adducts, favored in the gas phase (PyrHGu and OxHGu), and for charged adducts, favored in aqueous solution (PyrGuH and OxGuH). The DFT results are similar to the MP2 ones. The K_{HB} value for adduct between neutral species is greater for pyruvic than for oxamic acid in the gas phase, whereas a reverse situation takes place in aqueous solution, where the K_{HB} value for adduct between ionic species is smaller for pyruvate than for oxamate. Based on our results given in Table 5 we can conclude that the water molecules favor interactions of more polar oxamate with the guanidinium cation. Stronger interaction with this cation, a model of the arginine fragment of the LDH pocket, suggests that oxamate (inhibitor of LDH) has stronger binding properties than pyruvate (substrate of LDH). This observation may be essential for biotechnology. The use of oxamate for the selective biosepara-

Table 5. Gibbs free energies (ΔG_{HB} in kcal mol^{-1}) and formation constants (K_{HB}) for neutral adducts (PyrHGu and OxHGu) favored in the gas phase and for charged adducts (PyrGuH and OxGuH) favored in aqueous solution using the PCM model

Phase	Adduct	Method	ΔG_{HB}	K_{HB}
Gas	PyrHGu	MP2/6-31++G**	−7.0	$1.4\cdot10^5$
		B3LYP/6-31++G**	−6.9	$1.1\cdot10^5$
	OxHGu	MP2/6-31++G**	−5.3	$7.6\cdot10^3$
		B3LYP/6-31++G**	−5.7	$1.4\cdot10^4$
Water	PyrGuH	PCM//MP2/6-31++G**	−2.6	$7.9\cdot10^1$
		PCM//B3LYP/6-31++G**	−2.4	$5.2\cdot10^1$
	OxGuH	PCM//MP2/6-31++G**	−6.7	$7.8\cdot10^4$
		PCM//B3LYP/6-31++G**	−6.4	$4.5\cdot10^4$

tion of LDH or for analysis of biomaterials containing LDH may be more effective than the application of pyruvate.

CONCLUSIONS

Calculations performed for two types of bimolecular adducts (charged and neutral), which can model interaction of the substrate and inhibitor with LDH, show interesting change of adducts' preference and binding properties when going from the gas phase to aqueous solution. Neutral adducts (PyrHGu and OxHGu) are favored in the gas phase, whereas charged adducts (PyrGuH and OxGuH) predominate in aqueous solution. The substrate (pyruvic acid) of LDH has stronger binding properties than inhibitor (oxamic acid) in the gas phase (apolar environment), whereas a reverse situation takes place in aqueous solution (polar environment). The inhibitor of LDH (oxamate) has stronger binding properties than the substrate (pyruvate). Similarity of the DFT and MP2 results indicates additionally that the DFT method is sufficient for theoretical modeling of the substrate/inhibitor-LDH interactions.

Acknowledgements

M. M. was supported by a grant from the 'Homing' program of the Fundation for Polish Science (FNP) and MF EOG resources. MP2 and DFT calculations were carried out at the Interdisciplinary Centre for Molecular Modeling (ICM, Warsaw). MD symulations were conducted using the resources of 45-processor Beowulf cluster at the Faculty of Chemistry (University of Gdańsk) and the Informatics Center of the Metropolitan Academic Network (IC MAN, Gdańsk).

REFERENCES

[1] G. Zundel, Hydrogen bonds with large proton polarizability and proton-transfer processes in electrochemistry and biology, in *Advances in Chemical Physics*, vol. *111* (Eds.: I. Prigogine, S. A. Rice), Wiley, New York, 2000, pp. 1–217.
[2] T. E. Creighton, *Proteins: Structure and Molecular Properties*, Freeman, New York, **1993**.
[3] W. Saenger, *Principles of Nucleic Acid Structures*, Springer, New York, **1994**.
[4] R. P. Bell, *The Proton in Chemistry*, Cornell University Press, Ithaca, New York, **1959**.
[5] Eds.: E. Calvin, V. Gold, *Proton-Transfer Reactions*, Chapman & Hall, London, **1975**.
[6] E. D. Raczyńska, M. Darowska, *Pol. J. Chem.* **2002**, *76*, 1027–1035.
[7] E. D. Raczyńska, M. Darowska, M. K. Cyrański, M. Makowski, T. Rudka, J.-F. Gal, P.-C. Maria, *J. Phys. Org. Chem.* **2003**, *16*, 783–796.
[8] E. D. Raczyńska, T. Rudka, M. Darowska, I. Dąbkowska, J.-F. Gal, P.-C. Maria, *J. Phys. Org. Chem.* **2005**, *18*, 856–863.
[9] A. White, P. Handler, E. L. Smith, *Principles of Biochemistry*, McGraw-Hill, New York, **1968**.
[10] D. E. Corpet, G. F. Bories, *Drug Metab. Disposit.* **1987**, *15*, 925–927.
[11] L. Stryer, *Biochemistry*, W. H. Freeman, New York, **1995**.
[12] J. Koolman, K. H. Roehm, *Color Atlas of Biochemistry*, 2nd Edn, Thieme, **2005**.
[13] A. R. Clarke, D. B. Wigley, W. N. Chia, D. A. Barstaw, T. Atkinson, J. J. Holbrook, *Nature* **1986**, *32*, 699–702.
[14] E. Gawlita, P. Paneth, V. E. Anderson, *Biochemistry* **1995**, *34*, 6050–6058.
[15] R. K. Schmidt, J. E. Gready, *J. Mol. Struct. (Theochem)* **2000**, *498*, 101–112, and references cited therein.
[16] P. O'Carra, S. Barry, in *Methods in Enzymology* vol. 34 (Eds.: M. Jakoby, M. Wilchek), Academic Press, London, **1974**, 598–605.
[17] R. I. Brinkworth, C. J. Masters, D. J. Winzor, *Biochem. J.* **1975**, *151*, 631–636.
[18] E. A. Sevriukov, L. P. Evseev, *Vopr. Med. Khim.* **1994**, *40*, 23.
[19] I. Safarik, M. Safarikova, *J. Chromatogr.* **1999**, *B772*, 33–53.
[20] T. Larsen, *J. Diary Res.* **2005**, *72*, 209–216.
[21] K. Duczmal, *PhD Thesis. SGGW: Warszawa, Poland*, **2007**.
[22] K. Duczmal, M. Darowska, E. D. Raczyńska, *Vib. Spectrosc.* **2005**, *37*, 77–82.
[23] K. Duczmal, M. Hallmann, E. D. Raczyńska, J.-F. Gal, P.-C. Maria, *Pol. J. Chem.* **2007**, *81*, 1011–1020.
[24] E. D. Raczyńska, K. Duczmal, M. Hallmann, *Pol. J. Chem.* **2007**, *81*, 1655–1666.
[25] E. D. Raczyńska, K. Duczmal, M. Darowska, *Pol. J. Chem* **2005**, *79*, 689–697.
[26] E. D. Raczyńska, K. Duczmal, M. Darowska, *Vibr. Spectrosc.* **2005**, *39*, 37–45.
[27] K. Hanai, A. Kuwae, Y. Sugawa, K.-K. Kunimoto, S. Maeda, *J. Mol. Struct.* **2007**, *837*, 101–106.
[28] M. J. Adams, M. Buehner, K. Chandrasekhar, G. C. Ford, M. L. Hackert, A. Liljas, M. G. Rossmann, I. E. Smiley, W. S. Allison, J. Everse, N. O. Kaplan, S. S. Taylor, *Proc. Nat. Acad. Sci. USA* **1973**, *70*, 1968–1972.
[29] A. R. Clarke, A. D. B. Waldman, K. W. Hart, J. J. Holbrook, *Biochim. Biophys. Acta* **1985**, *829*, 397–407.
[30] A. R. Clarke, T. Atkinson, J. J. Holbrook, *Trends Biochem. Sci.* **1989**, *14*, 101–105.
[31] Z. Wu, C. Fenselau, *J. Am. Soc. Mass Spectrom.* **1992**, *3*, 863–866.
[32] E. P. Hunter, S. G. Lias, *J. Phys. Chem. Pef. Data* **1998**, *27*, 413–656.
[33] D. D. Perrin, *Dissociation Constants of Organic Bases in Aqueous Solution*, *1965*, Supplement, Butterworths, London, **1972**.
[34] Y. Y. G. Schlippe, L. Hedstrom, *Arch. Biochem. Biophys.* **2005**, *433*, 266–278.
[35] P. Retailleau, N. Colloc'h, D. Vivarčs, F. Bonneté, B. Castro, M. El Hajji, T. Prangé, *Acta Cryst.* **2005**, *D61*, 218–229.
[36] C. Möller, M. S. Plesset, *Phys. Rev.* **1934**, *46*, 618–622.
[37] J. A. Pople, J. S. Brinkley, R. Seeger, *Int. Quantum Chem. Symp.* **1976**, *10*, 1–19.
[38] R. G. Par, W. Yang, *Density Functional Theory of Atoms and Molecules*, Oxford University Press, New York, **1989**.
[39] A. D. Becke, *J. Chem. Phys.* **1993**, *98*, 5648–5652.
[40] C. Lee, W. Yang, R. G. Parr, *Phys. Rev. B* **1988**, *37*, 785–789.
[41] W. J. Hehre, L. Radom, PvR. Schleyer, J. A. Pople, *Ab initio Molecular Theory*, Wiley, New York, **1986**.
[42] S. Miertuš, E. Scrocco, J. Tomasi, *J. Chem. Phys.* **1989**, *55*, 117–129.
[43] M. Szafran, M. M. Karelson, A. R. Katritzky, J. Koput, M. C. Zerner, *J. Comput. Chem.* **1993**, *14*, 371–377.
[44] R. Cammi, J. Tomasi, *J. Comput. Chem.* **1995**, *16*, 1449–1458.
[45] C. S. Pomelli, J. Tomasi, *Theor. Chem. Acc.* **1997**, *96*, 39–43.
[46] S. F. Boys, F. Bernardi, *Mol. Phys.* **1970**, *19*, 553–560.
[47] S. Simon, M. Duran, J. J. Dannenberg, *J. Chem. Phys.* **1996**, *105*, 11024–11031.
[48] M. J. Frisch, G. W. Trucks, H. B. Schlegel, G. E. Scuseria, M. A. Robb, J. R. Cheeseman, V. G. Zakrzewski, J. A. Montgomery, Jr, R. E. Stratmann, J. C. Burant, S. Dapprich, J. M. Millam, A. D. Daniels, K. N. Kudin, M. C. Strain, O. Farkas, J. Tomasi, V. Barone, M. Cossi, R. Cammi, B. Mennucci, C. Pomelli, C. Adamo, S. Clifford, J. Ochterski, G. A. Petersson, P. Y. Ayala, Q. Cui, K. Morokuma, D. K. Malick, A. D. Rabuck, K. Raghavachari, J. B. Foresman, J. Cioslowski, J. V. Oritz, A. G. Baboul, G. Liu, A. Liashenko, P. Piskorz, I. Komaromi, R. Gomperts, R. L. Martin, D. J. Fox, T. Keith, M. A. Al-Laham, C. Y. Peng, A. Nanayakkara, M. Challacombe, P. M. W. Gill, B. G. Johnson, W. Chen, M. W. Wong, J. L. Andres, C. Gonzalez, M. Head-Gordon, E. S. Replogle, J. A. Pople, *Gaussian 98*, Gaussian, Inc., Pittsburgh PA, **1998**.
[49] W. L. Jorgensen, J. Chandrasekhar, J. D. Madura, R. W. Impey, M. L. Klein, *J. Chem. Phys.* **1983**, *79*, 926–935.
[50] T. Darden, D. York, L. Pedersen, *J. Chem. Phys.* **1993**, *98*, 10089–10092.
[51] D. A. Case, D. A. Pearlman, J. W. Caldwell, T. E. Chaetham, III, J. Wang, W. S. Ross, C. L. Simmerling, T. A. Darden, K. M. Merz, R. V. Stanton, A. L. Cheng, J. J. Vincent, M. Crowley, V. Tsui, H. Gohlke, R. J. Radmer, Y. Duan, J. Pitera, I. Massova, G. L. Seibel, U. C. Singh, P. K. Weiner, P. A. Kollman, *AMBER 7.0*, University of California, San Francisco, **2002**.
[52] M. W. Schmidt, K. K. Baldridge, J. A. Boatz, S. T. Elbert, M. S. Gordon, J. A. Jensen, S. Koseki, N. Matsunaga, K. A. Nguyen, S. Su, T. L. Windus, M. Dupuis, J. A. Montgomery, *J. Comput. Chem.* **1993**, *14*, 1347–1363.

[53] C. I. Bayly, P. Cieplak, W. D. Cornell, P. A. Kollman, *J. Phys. Chem.* **1993**, *97*, 10269–10280.
[54] S. Kumar, J. M. Rosenberg, D. Bouzida, R. H. Swendsen, P. A. Kollman, *J. Comput. Chem.* **1995**, *16*, 1339–1350.
[55] S. Kumar, D. Bouzida, R. H. Swendsen, P. A. Kollman, J. M. Rosenberg, *J. Comput. Chem.* **1992**, *13*, 1011–1021.
[56] S. S. Tavale, L. M. Pant, A. B. Biswas, *Acta Cryst.* **1961**, *14*, 1281–1286.
[57] W. Rach, G. Kiel, G. Gattow, *Z. Anorg. Allg. Chem.* **1988**, *563*, 87–95.
[58] B. Beagley, R. W. H. Small, *Proc. R. Soc. (London) A* **1963**, *275*, 469–491.
[59] A. M. O'Connell, A. I. M. Rae, E. N. Maslen, *Acta Cryst.* **1966**, *21*, 208.
[60] C. B. Aakeröy, D. P. Hughes, M. Nieuwenhuyzen, *J. Am. Chem. Soc.* **1996**, *118*, 10134–10140.
[61] X. Yang, G. Orlova, X. J. Zhou, K. T. Leung, *Chem. Phys. Lett.* **2003**, *380*, 34–41, and references cited therein.
[62] I. D. Reva, S. G. Stephanian, L. Adamowicz, R. Fausto, *J. Phys. Chem A* **2001**, *105*, 4773–4780, and references cited therein.
[63] R. Kakkar, M. Pathak, N. M. Radhika, *Org. Biomol. Chem.* **2006**, *71*, 3727.
[64] C. van Alsenoy, L. Schäfer, K. Siam, J. D. Ewbank, *J. Mol. Struct. (Theochem)* **1989**, *187*, 271–2283.
[65] J. Murto, T. Raaska, H. Kunttu, M. Räsänen, *J. Mol. Struct. (Theochem)* **1989**, *200*, 93–101.
[66] P. Tarakeshwar, S. Manogram, *J. Mol. Struct. (Theochem)* **1998**, *430*, 51–56.
[67] C. Chen, S.-F. Shyu, *J. Mol. Struct. (Theochem)* **2000**, *503*, 201–211.
[68] Z. Zhou, D. Du, A. Fu, *Vibr. Spectrosc.* **2000**, *23*, 181–186.
[69] K. Harata, N. Sakabe, J. Tanaka, *Acta Cryst.* **1977**, *B33*, 210–212.
[70] F. Wallace, E. Wagner, *Spectrochim. Acta* **1978**, *34A*, 589–606.
[71] G. N. R. Tripath, J. E. Katon, *Spectrochim. Acta* **1979**, *35A*, 401–407.
[72] I. Wolfs, H. O. Desseyn, *Spectrochim. Acta* **1995**, *51A*, 1601–1615.
[73] K.-M. Marstokk, H. Møllendal, *J. Mol. Struct.* **1974**, *20*, 257–267.
[74] E. D. Raczyńska, M. K. Cyrański, M. Gutowski, J. Rak, J.-F. Gal, P.-C. Maria, M. Darowska, K. Duczmal, *J. Phys. Org. Chem.* **2003**, *16*, 91–106, and references cited therein.
[75] A. Gobbi, G. Frenking, *J. Am. Chem. Soc.* **1993**, *115*, 2362–2372.
[76] W. Jones, *Trans Faraday Soc.* **1959**, *55*, 524.
[77] H. F. Allen, J. E. Davies, J. J. Galloy, O. Johnson, O. Kennard, E. M. McRae Mitchell, G. F. Mitchell, J. M. Smith, D. G. J. Watson, *J. Chem. Inf. Comput. Sci.* **1991**, *31*, 187–204.
[78] F. H. Allen, S. Bellard, M. D. Brice, B. A. Cartwright, A. Doubleday, H. Higgs, T. Hummelink, B. G. Hummelink-Peters, O. Kennard, W. D. S. Motherwell, J. R. Rodgers, D. G. Watson, *Acta Crystallogr.* **1979**, *B35*, 2331–2339.
[79] E. D. Raczyńska, M. Hallmann, K. Duczmal, *Pol. J. Chem.* **2008**, *82*, 1077–1090.
[80] B. Kratochvíl, J. Ondráček, J. Krechl, J. Hašek, *Acta Cryst.* **1987**, *C43*, 2182–2184.
[81] D. D. Bray, N. Slatery, C. S. Russell, *Int. J. Pept. Protein Res.* **1984**, *24*, 414–418.
[82] A. Zafar, R. Melendez, S. J. Geib, A. D. Hamilton, *Tetrahedron* **2002**, *58*, 683–690.
[83] D. S. Eggleston, D. J. Hodgson, *Int. J. Pept. Protein Res.* **1985**, *25*, 242–253.
[84] J. Singh, J. M. Thornton, M. Snarey, S. F. Campbell, *FEBS Lett.* **1987**, *224*, 161–171.
[85] E. D. Raczyńska, J.-F. Gal, P.-C. Maria, K. Zientara, M. Szeląg, *Anal. Bioanal. Chem.* **2007**, *389*, 1365–1380.
[86] A. D. Headly, S. D. Starnes, *Trends Org. Chem.* **1998**, *7*, 75–84.
[87] L. Sobczyk, S. J. Grabowski, T. M. Krygowski, *Chem. Rev.* **2005**, *105*, 3513–3560, and references cited therein.
[88] A. Masunov, T. Lazaridis, *J. Am. Chem. Soc.* **2003**, *125*, 1722–1730.
[89] J. Makowska, M. Makowski, A. Giełdoń, A. Liwo, L. Chmurzyński, *J. Phys. Chem. B* **2004**, *108*, 12222–12230.
[90] X. Rozanska, Ch. Chipot, *J. Chem. Phys.* **2000**, *122*, 9691–9694.
[91] M. Makowski, A. Liwo, K. Maksimiak, J. Makowska, H. A. Scheraga, *J. Phys. Chem. B* **2007**, *111*, 2917–2924.
[92] M. Makowski, E. Sobolewski, C. Czaplewski, A. Liwo, S. Ołdziej, H. A. Scheraga, *J. Phys. Chem. B* **2007**, *111*, 2925–2931.